ARMY RESEARCH LABORATORY

Spectroscopic Studies of the Gas-Phase ArCH(D) Complexes: I. Detection and Analysis of B-X Electronic Transitions of ArCH by Laser-Induced Fluorescence

M. J. McQuaid
R. C. Sausa
G. W. Lemire
A. J. Kotlar

ARL-TR-1220 October 1996

NOTICES

Destroy this report when it is no longer needed. DO NOT return it to the originator.

Additional copies of this report may be obtained from the National Technical Information Service, U.S. Department of Commerce, 5285 Port Royal Road, Springfield, VA 22161.

The findings of this report are not to be construed as an official Department of the Army position, unless so designated by other authorized documents.

The use of trade names or manufacturers' names in this report does not constitute indorsement of any commercial product.

REPORT DOCUMENTATION PAGE

Form Approved
OMB No. 0704-0188

1. AGENCY USE ONLY *(Leave blank)*	2. REPORT DATE	3. REPORT TYPE AND DATES COVERED
	November 1996	Final, Jan 93 - Jan 95

4. TITLE AND SUBTITLE
Spectroscopic Studies of the Gas-Phase ArCH(D) Complexes: I. Detection and Analysis of B-X Electronic Transitions of ArCH by Laser-Induced Fluorescence

5. FUNDING NUMBERS
PR: 1L161102AH43

6. AUTHOR(S)
M. J. McQuaid, R. C. Sausa, G. W. Lemire, and A. J. Kotlar

7. PERFORMING ORGANIZATION NAME(S) AND ADDRESS(ES)
U.S. Army Research Laboratory
ATTN: AMSRL-WT-PA
Aberdeen Proving Ground, MD 21005-5066

8. PERFORMING ORGANIZATION REPORT NUMBER
ARL-TR-1220

9. SPONSORING/MONITORING AGENCY NAMES(S) AND ADDRESS(ES)

10.SPONSORING/MONITORING AGENCY REPORT NUMBER

11. SUPPLEMENTARY NOTES

12a. DISTRIBUTION/AVAILABILITY STATEMENT
Approved for public release; distribution is unlimited.

12b. DISTRIBUTION CODE

13. ABSTRACT *(Maximum 200 words)*

Gas-phase argon-methylidyne (ArCH) van der Waals (vdW) complexes have been detected spectroscopically by laser-induced fluorescence (LIF) near CH $B^2\Sigma^- - X^2\Pi_r$ (0,0) and (1,0) transitions. They are formed in a supersonic free-jet expansion of argon seeded with CH radicals generated by the 248-nm photolysis of $CHBr_2Cl$. The LIF spectra reveal a number of rovibronic bands that are assigned to stretching and/or bending motions of the ArCH complex. From the spectra, lower limits for the ground and exited state binding energies are estimated. Analysis of the rotational energy level structure based on combination differences and computer simulations of eight of the rovibronic bands yields an average ground state value of $B''_{av} = 0.174 \pm 0.004$ cm^{-1} and excited state constants ranging from $B' = 0.086 - 0.116$ cm^{-1}. This indicates that the ArCH vdW bond is lengthened considerably upon electronic excitation. A splitting of the ground state rotational energy levels is observed that is related to the nature of the intermolecular potential and Coriolis coupling. Based on the rovibronic structure of the ArCH bands and a hindered internal rotational model describing the interaction of $Ar(^1S_o)$ atom with a CH monomer, a linear equilibrium geometry is inferred for the excited state and a T-shaped geometry for the ground state.

14. SUBJECT TERMS
van der Waals (vdW) complex, laser-induced fluorescence (LIF), methylidyne radical, spectroscopy, rotational analysis, and supersonic expansion

15. NUMBER OF PAGES
30

16. PRICE CODE

17. SECURITY CLASSIFICATION OF REPORT	18. SECURITY CLASSIFICATION OF THIS PAGE	19. SECURITY CLASSIFICATION OF ABSTRACT	20. LIMITATION OF ABSTRACT
UNCLASSIFIED	UNCLASSIFIED	UNCLASSIFIED	UL

INTENTIONALLY LEFT BLANK.

ACKNOWLEDGMENTS

The author's wish to thank Professors M. Heaven, Emory University, and P. Dagdigian, John Hopkins University, for their critical review of the manuscript. We would also like to thank Professor Heaven for providing an explanation for the nature of the splitting in the ground state rotational levels of the ArCH complex and for performing supporting calculations. Drs. N. Garland and H. Nelson, U.S. Naval Research Laboratory, are gratefully acknowledged for providing us with various CH precursor compounds and their UV-VIS absorption spectra. This work was supported in part by the U.S. Army Research Laboratory (ARL) Combustion Research Mission Program. Purchase of equipment through the Productivity Capital Investment Program (R. C. Sausa) and support from the NRC Postdoctoral Research Associate Program (G. W. Lemire) are also gratefully acknowledged.

INTENTIONALLY LEFT BLANK.

TABLE OF CONTENTS

INTENTIONALLY LEFT BLANK.

LIST OF FIGURES

LIST OF TABLES

INTENTIONALLY LEFT BLANK.

1. INTRODUCTION

The methylidyne radical (CH) has been the subject of numerous spectroscopic and kinetic studies [1–3]. This interest stems from the fact that this radical is an important intermediate in flame and combustion processes [4, 5], and plays a prominent role in interstellar and atmospheric chemistry [6, 7]. Modeling the dynamics of these varied environments requires the measurement and/or theoretical calculation of numerous bimolecular reaction rates for many different collisional partners. A prerequisite for performing the theoretical calculations is the determination of the intermolecular potential surface on which the interaction takes place. The potential function needed to describe the intermolecular surface is quite difficult to generate, particularly for reactive collisions [8, 9]. However, insight into the construction of such surfaces can be provided by studying the collisions between a radical and a "nonreactive" rare-gas (RG) atom. Characterization of bound regions of these surfaces is facilitated via the spectroscopic investigations of van der Waals (vdW) complexes [10, 11].

Open-shell diatom-RG atom vdW complexes have been the focus of numerous experimental and theoretical investigations [11–42]. In addition to the interest in understanding the collisional dynamics and structure of weakly bound systems, these complexes have been recognized as model systems for studying unique angular momentum coupling cases [21, 25, 28, 32, and 42]. The fact that these systems are small enough for accurate theoretical calculations has added to the interest in these species. However, unlike their closed-shell-RG counterparts, only a few systems have been detected spectroscopically. Most of the experimental and theoretical activity has surrounded RG-OH [11–34] and, to a lesser degree, RG-NO [35–40]. Recent experimental observations of RG-CN [41] and Ar-NH [42] have also been reported.

RG-OH complexes were first observed spectroscopically by Goodman and Brus in cryogenic noble gas matrices [12]. They were interested in understanding hydrogen bonding and how it compared with other weak chemical interactions. Based on simple molecular orbital arguments, the bonding in the RG-OH molecule was assumed to be through the hydrogen end of the molecule. Recent theoretical calculations by Degli-Esposti and Werner [29] corroborate this assumption. They determine, however, that bonding through the oxygen end is only slightly higher in energy. The results from recent high-resolution spectroscopic studies provide further confirmation for the predicted potential surface [21]. In the case of CH, hydrogen bonding is not expected to play a significant role since the carbon atom is less electronegative than the oxygen atom. Thus, one cannot intuitively predict the geometric configuration of RG-CH complexes.

The wealth of spectroscopic information on the RG-OH systems, particularly the Ar-OH complex, has prompted a considerable number of theoretical studies. Ab initio calculations have been carried out by Degli-Esposti and Werner [29] in order to construct intermolecular potential surfaces for the Ar-OH complex associated with OH ground ($X^2\Pi_i$) and excited ($A^2\Sigma^+$) states. These surfaces were then used by Chakravarty and Clary [30] to simulate electronic and infrared spectra. The results of other studies have yielded perturbation schemes [33, 34] to explain parity splitting in both the Ar-OH $X^2\Pi_{1/2}$ and $X^2\Pi_{3/2}$ states, as well as, spin-orbit predissociation rates [33]. Dubernet, Flower, and Hutson [32] developed a general theory, which was extended by Chang and coworkers [21], to derive information about the potential energy surface based on analysis of the energy level structure for various coupling schemes. Although the ArOH and NeOH complexes were used as examples, this theory is general and applies to ArCH.

In the present work, we report the detection of gas-phase ArCH complexes. The complexes were excited near the CH $B^2\Sigma^- - X^2\Pi_r$ (0,0) and (1,0) transitions and fluorescence was monitored. The rotational energy level structure of eight bands is analyzed. In addition, the rovibronic energy level structure is analyzed based on a hindered internal rotation model [34, 21] to explain the nature of the observed splittings of the ground state rotational levels, and to infer both excited and state geometries. Lower limits for the ground and excited binding energies are also reported.

2. EXPERIMENTAL

The molecular beam apparatus employed in these experiments has been described previously [26]. Briefly, the ArCH complexes were formed by photolyzing chlorodibromomethane, $CHBr_2Cl$ (Aldrich, 98%), seeded in a supersonic free-jet expansion. The expansion of argon (Spectra Gases Inc., 99.995%) was controlled via a pulsed valve (R. M. Jordan Co., PVS) operated at 10 Hz. The backing pressure was nominally 100–120 psi. Photolysis producing CH radicals was achieved with approximately 25 mJ/pulse of 248-nm radiation (Lambda Physik, EMG 150MSC). The photolysis beam was directed collinear to the molecular beam and focused with a 1-meter lens into an extender channel mounted in front of the valve. A delay generator was employed to synchronize the firing of the photolysis pulse and the gas pulse. The mixture was photolyzed approximately 6–8 μs following the opening of the valve - the peak of the gas load in the extender channel. The ArCH complexes were probed normal to the molecular beam, 3–5 mm in front of the extender channel, using an XeCl excimer pumped dye laser system (Lumonics Hyper Ex-400 and Hyper Dye-300). Laser dyes PBD and BBQ were used to generate tunable radiation in ranges

from 360–367 nm and 385–392 nm, respectively. These ranges include resonant excitation frequencies of the CH $A^2\Sigma^- - X^2\Pi_r$ (0,0) and (1,0) transitions. At these wavelengths, the laser line width is approximately 0.08 cm^{-1}. The probe energies employed were nominally 1–4 mJ/pulse.

The fluorescence signal was focused onto the entrance slit of a 0.25-m monochromator (McPherson, Model 218) that was operated as a broadband filter. The emission from the ArCH transitions excited in the region of the CH $B^2\Sigma^- - X^2\Pi_r$ (0,0) band was monitored near the (0,0) transition at 386.1 nm. Those excited near the (1,0) band were monitored both at 364.5 and 404.0 nm. These wavelengths correspond to the CH $B^2\Sigma^- - X^2\Pi_r$ (1,0) and (1,1) transitions, respectively. A photomultiplier tube (EMI 9789QA) was used for signal detection. The signal was directed to a gated integrator (Stanford Research Systems) and displayed on a 350-MHz digital oscilloscope (LeCroy 9420). For data acquisition, a PC was interfaced to the boxcar integrator via a commercial system interface package (Stanford Research Systems).

The multiphoton UV photolysis of $CHBr_2Cl$ has been demonstrated to be a good source of the CH radical [3]. However, the large energy fluxes required for the multiphoton dissociation process results in the formation of other fragments, which can obscure the LIF spectra of the ArCH complexes. During the initial phase of this investigation, the presence of an unknown band system or systems, probably belonging to either CCl or HCCl, was observed. These bands were present regardless of whether helium, neon, or argon was used as the carrier gases. Fortunately, these bands did not appear in the region of the ArCH spectra. The band systems assigned to ArCH were present only when argon was used as the carrier gas, and under jet-cooling conditions.

3. RESULTS/DISCUSSION

Presented in Figures 1a and 1b are the LIF spectra exited near the CH $B^2\Sigma^- - X^2\Pi_r$ (0,0) and (1,0) bands, respectively. Neither spectrum has been corrected for the variation in laser intensity or detection sensitivity. The features in Figure 1b at higher energy suffer from a decrease in intensity as a result of a dropoff in the gain profile of the dye. The strong features labeled $P_1(1)$, $P_2(1)$, $Q_1(1)$, $Q_2(2)$, $R_1(1)$, and $R_2(1)$ are CH B–X (0,0) and (1,0) rotational lines. These lines provided a basis for calibrating the spectra [1, 43]. To the blue of these sharp lines is a collection of broad, red-shaded features associated with the ArCH complex. The features located at lower energies (**A–G**) are resolvable under high resolution. Those at higher energies (**H–K[L]**) are more intense, broader, show little or no resolvable features at higher

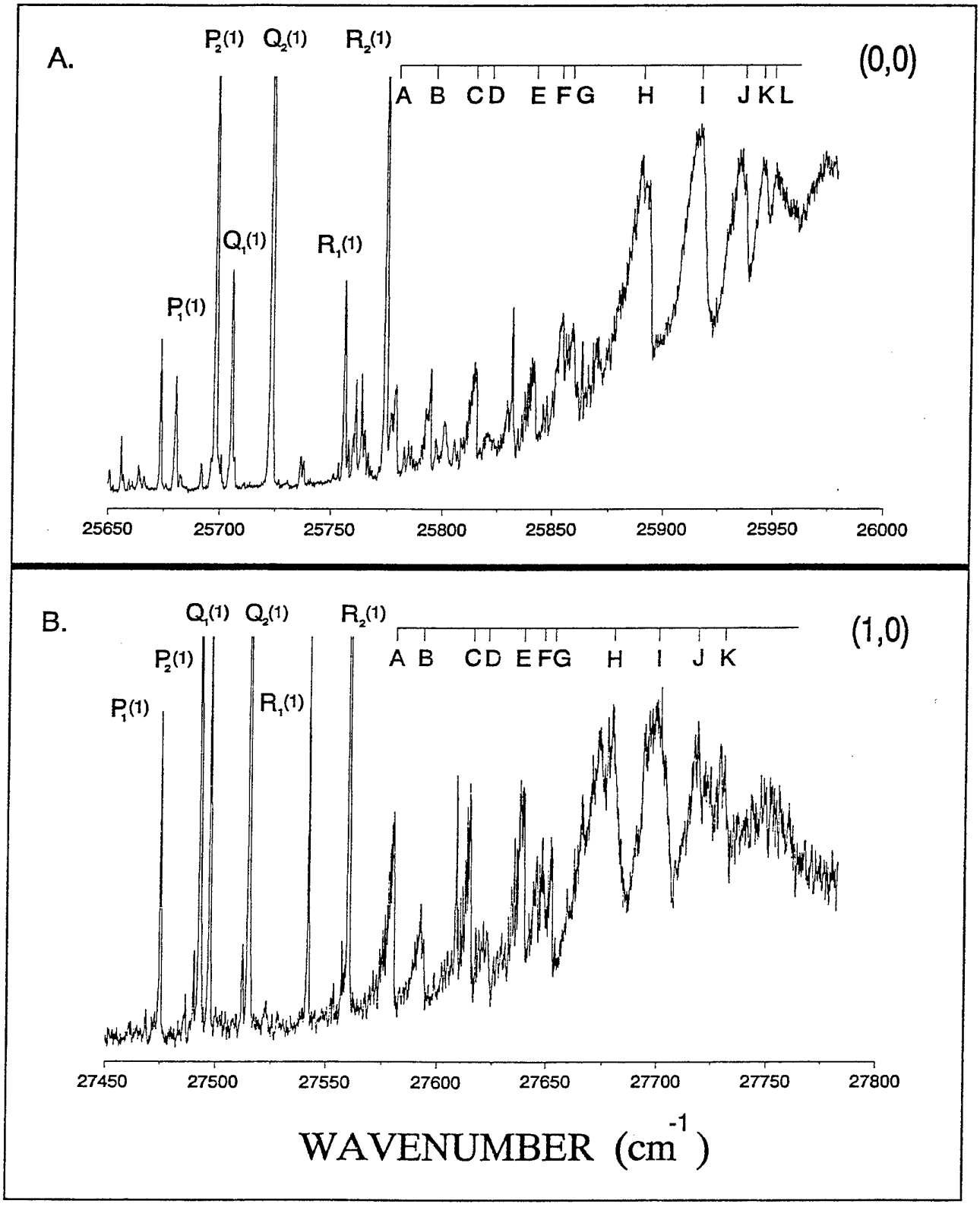

Figure 1. Laser-induced fluorescence spectra of ArCH excited near CH $B^2\Sigma^- - X^2\Pi_r$ (0,0) and (1,0) transitions.

resolution, and converge into a continuum. The lack of resolvable structure indicates that these bands are associated with transitions to metastable excited state levels. This is supported by an estimate of the dissociation energy calculated below. A listing of the band head positions assigned to the ArCH complex is presented in Table 1.

Table 1. Band Head Positions (in cm^{-1}) of Experimentally Observed ArCH Spectral Features Near the CH $B^2\Sigma^- - X^2\Pi_r$ (0,0) and (1,0) Transitions[a]

Band	(0,0)	(1,0)
	G	G
A	25779.0	27580.0
B	25794.6	27593.4
C	25815.3	27614.9
D	25820.9	27623.9
E	25841.9	27639.4
F	25854.3	27648.1
G	25859.2	27652.5
H	25892.0	27679.0
I	25916.0	27701.0
J	25935.0	27718.0
K	25945.0	27728.0
L	25951.0	—

[a] The experimental uncertainty in the band head positions of features A–G is ±0.2 cm^{-1}. For features H–I, the uncertainty in reporting the band head position is ±2 cm^{-1}.

3.1 Rotational Analysis. Rotationally resolved spectra have been recorded for ten of the features shown in Figures 1a and 1b. Six of these bands were fully analyzed, and two bands were characterized from a partial analysis based on transitions near the band head. The remaining two bands were not analyzed because of either significant overlap with CH transitions or a lack of a recognizable branch structure. Good empirical fits of all the bands analyzed were obtained using a model based on Σ-Σ type transitions. In this model, the term values for both ground and excited state rotational energy levels were obtained using the expressions:

$$F_1(N) = BN(N+1) - DN^2(N+1)^2 + 0.5\gamma N \quad (1a)$$

$$F_2(N) = BN(N+1) - DN^2(N+1)^2 - 0.5\gamma(N+1), \quad (1b)$$

where N is an integer quantum number, B is the effective "rigid rotor" constant, and D is the coefficient for centrifugal distortion. The terms containing γ were included to allow for spin-rotation coupling in the excited state, and a phenomenologically observed splitting in the ground state rotational levels. Justification for these functional forms is provided in the latter part of this report. The selection rule $\Delta N = \pm 1$ leads to six branches which we label R_1, R_2, R_{21}, P_1, P_2, and P_{12}. A schematic diagram for the energy levels and transition types assumed in this model is presented in Figure 2.

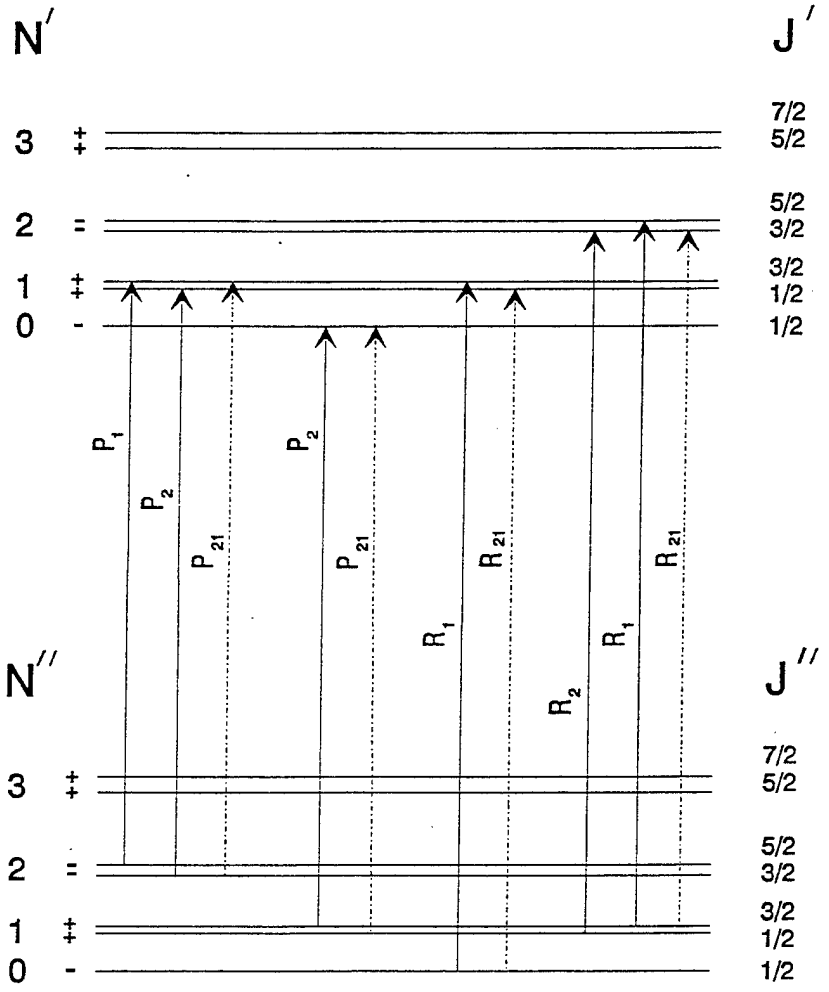

Figure 2. Rotational energy level diagram for Σ-Σ transitions.

Combination differences based on trial assignments were used to obtain initial estimates for B′, B″, and γ″. In principle, both γ′ and γ″ could be determined directly from combination differences. However, limited by resolution at low *N* values and signal-to-noise levels at high N values, the combination differences did not yield precise enough values for this purpose. *A priori*, it was considered that significant splitting of the excited state levels was unlikely. Chang and coworkers [21] have shown that the spin-rotation constant of a complex correlating with a $^2\Sigma$ monomer, and having no projected vibrational angular momentum along the intermolecular axis, scales with the mass. For the ArCH complex, this relationship may be expressed as,

$$\gamma\,(\mathrm{ArCH}) = \gamma\,(\mathrm{CH}) \times [B\,(\mathrm{ArCH})/B\,(\mathrm{CH})], \tag{2}$$

where γ and B are the spectroscopic constants defined previously. Using the known values of $\gamma = 0.0285$ cm^{-1}, $B = 12.6$ cm^{-1} for CH $B^2\Sigma^-$, and a value of $B \approx 0.1$ cm^{-1} for ArCH, γ (ArCH) is expected to be on the order of 2.0×10^{-4} cm^{-1}. The splitting associated with this term would not be observed at the resolution of these experiments. Thus, we initially assumed that γ′ was negligible.

To verify assignments, obtain improved estimates of the rotational constants, and determine band origins, graphical simulations were generated using a multivariable computer program based on the energy level expressions and selection rules given previously, and Σ-Σ line strengths. The program variables included the rotational constants of the ground and excited states, the band origin (ν_{00}), the transition line width, and the population of the ground state levels based on Boltzmann (temperature) distribution. The first iteration in obtaining estimates of the rotational constants based on this model involved nonlinear least-squares fits of bands **A**, **B**, and **C**, of Figure 1a and bands **A** and **C** of Figure 1b. The average values of B″ and γ″ obtained from these fits were then used in fits in which only B′, γ′, and ν_{00} were varied. Using a convergence criteria of four significant figures, γ′ was found to be negligible in all of the bands analyzed. A final fit, where γ′ was set equal to zero and the average ground state constants were used, provided a consistent set of excited state constants and band origins. A slight qualitative improvement in the final fits could be obtained by including a correction for centrifugal distortion. However, the correction term was $\leq 5 \times 10^{-6}$ cm^{-1} and not statistically significant. A comparison of the band labeled **A** in Figure 1b and its graphical simulation is shown in Figure 3. The values obtained for excited state rotational constants and band origins, together with their uncertainties, are reported in Table 2. It should be noted that the simulation of the band positions is indifferent to the sign of γ″. A sign change does

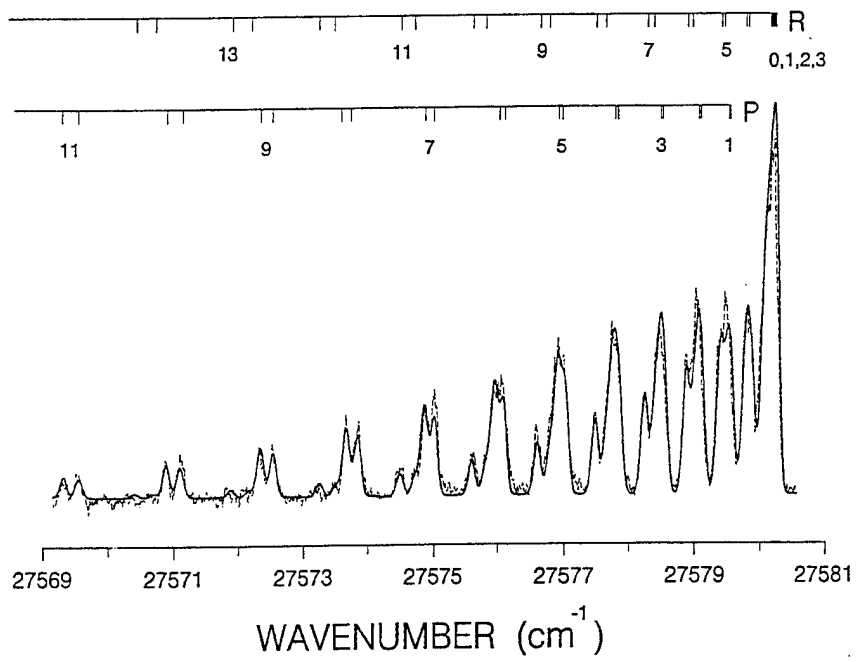

Figure 3. Laser-induced fluorescence spectrum (--) and simulation (-) of the ArCH B-X (1,0,0) band. A nonlinear least-squares fit of the data yields a value of 27579.9 cm^{-1} for the band origin, and values of $B' = 0.114 \pm 0.005$ cm^{-1} and $B'' = 0.174 \pm 0.005$ cm^{-1} for the rotational constants.

Table 2. Calculated Rotational Constants and Band Origins Associated With Electronic Excitation of CH $B^2\Sigma^- - X^2\Pi_r$ (0,0) and (1,0) Transitions[a]

(0,0)				
Band	Assignment	ν' (cm^{-1})[b]	B' (cm^{-1})[c]	R'_e (Å)
A	$(0,0^0,0)$	25778.6	0.113	3.90
B	$(0,1^0,0)$	25794.3	0.116	3.85
C	$(0,0^0,1)$	25815.1	0.102	4.10
E	$(0,0^0,2$	25842.1	0.086	4.47
(1,0)				
A	$(1,0^0,0)$	27579.9	0.114	3.88
C	$(1,0^0,1)$	27615.0	0.102	4.10
E	—	27639.5	0.099[d]	4.17
F	—	27652.3	0.099[d]	4.17

[a] The average values of the ground state rotational constants are $B''_{av} = 0.174 \pm 0.004$ (2SD) ($R'_e = 3.13$ Å) and $\gamma''_{av} = 0.021 \pm 0.004$ (2SD).
[b] Experimental uncertainty of ± 0.1 cm^{-1}.
[c] Experimental uncertainty of ± 0.004 cm^{-1}.
[d] Based on partial rotational analysis near band head.

create a slight difference in the simulation's intensity distribution. However, the empirical nature of the line strength factors in the simulation program, and the lack of experimental data necessary to rigorously correct the experimentally determined line intensities, preclude us from drawing a conclusion based on the line intensities.

The B values obtained here are effective constants for a near-prolate top [B_{eff} = (B+C)/2]. This parameter depends mainly on the vibrationally averaged distance (R_o) between the CH center of mass and the Ar atom. The average ground state B''_{av} value corresponds to an average R_o value of 3.13 Å. The B′ values are all significantly smaller, indicating a lengthening of the internuclear distance upon electronic excitation. The R_v' values range from 3.85 Å to 4.47 Å. For comparison, the average bond length of ground state ArOH was found to be approximately 3.76 Å. In the complexes associated with OH $A^2\Sigma^+$ (v = 0) and (v = 1) excited states, values ranging from 3.04 to 3.63 Å and 3.11 to 3.36 Å, respectively, have been reported [18].

3.2 Vibrational Analysis. The assignment of the fundamental modes of vibration of the ArCH $B^2\Sigma^-$ state is based on the B′ values derived from the rotational analysis and the assumption that the lowest vibrational level of the excited state is observed. As observed in cases of ArOH and NeCN, the excitation of a quantum of ArCH stretch is accompanied by a large drop in B′, while the excitation of bending quantum generally does not decrease B′. This occurs because the vibrationally averaged ArCH bond length increases substantially more for the excitation of a stretch than a bend. The modes are labeled (v_1, r^ρ, v_s), where v_1 is the quanta of C-H stretch, r is the quanta of bend/hindered internal rotation of CH with respect to Ar, ρ is the projection of the bend on the intermolecular axis of the complex, and v_s is the quanta of ArCH stretch.

In Figure 1a, the lowest energy band (feature A) observed for the complex is at 25778.6 cm^{-1}. The intensity distribution of the observed bands suggests that lower energy transitions of the complex would be observed if they existed. Thus, the A band is attributed to the lowest vibrational level of the excited electronic state of the complex ($0,0^0,0$). The bands at 25794.3 cm^{-1} and 25815.1 cm^{-1} (features B and C) are assigned to the first fundamental bend ($0,1^0,0$) and stretch ($0,0^0,1$) of the complex. The ($0,1^0,0$) band is the only band which involves excitation of a bending level for which a full rotational analysis was completed. Chang and coworkers [25] have described the significant coupling differences between ArOH vibronic states which have a projection on the internuclear axis (ρ = 1) and those which do not (ρ = 0).

The similarity of the observed bands assigned as $(0,0^0,0)$ and $(0,1^0,0)$ suggests that the coupling in the excited state is the same in both cases and indicates that $\rho = 0$ for the vibronic band.

The band labeled **E** in Figure 1a is assigned as $(0,0^0,2)$, and those labeled **A, C, E,** and **F** in Figure 1b are assigned $(1,0^0,0)$, $(1,0^0,1)$, $(1,1^{\rho'},1)$, and $(1,1^{\rho''},1)$, respectively. The feature labeled **B**, in Figure 1b, at 27593.4 cm^{-1} could not be fully analyzed and is not assigned.

3.3 Binding Energies. Figure 4 presents a Birge-Sponer plot of the vibrational energy level separations in the stretching coordinate as the ArCH B state. The extrapolation of this plot provides an estimate of the B state binding energy (90 cm^{-1}) and would suggest the existence of $(0,0^0,3)$ and $(0,0^0,4)$ levels. However, no rotationally resolved bands that can be associated with the $(0,0^0,3)$ or $(0,0^0,4)$ level are observed. A firm lower limit of the B state binding energy is provided by the $(0,0^0,2) - (0,0^0,0)$ separation - 63.5 cm^{-1}.

The ground state binding energy (D_o'') of Ar-CH may be calculated using the equation,

$$D_o''\,(\text{Ar-CH}, v'' = 0) - D_o'\,(\text{Ar-CH}, v' = 0) = \nu_{00}\,(\text{ArCH}) - \nu_{00}\,(\text{CH}). \qquad (3)$$

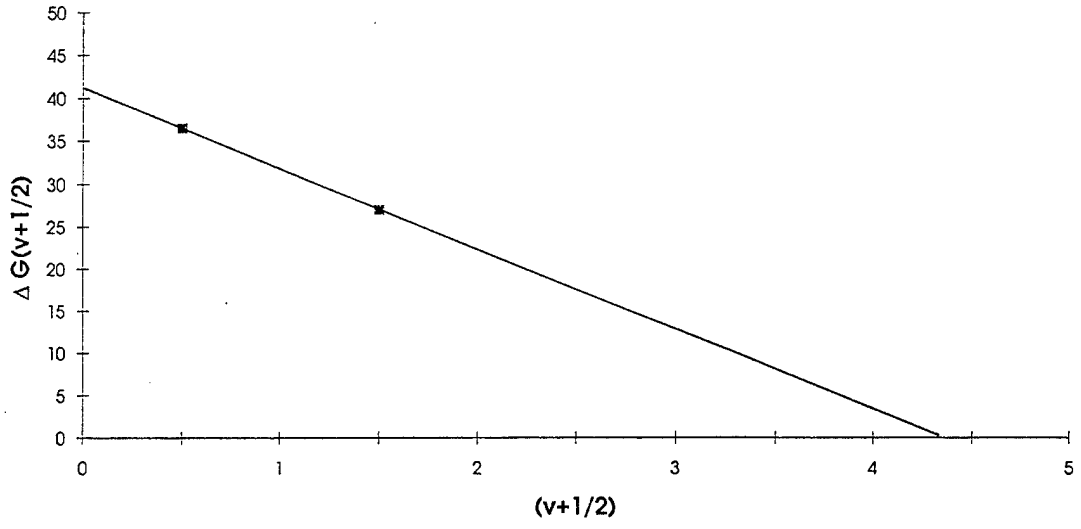

Figure 4. Birge-Sponer extrapolation of vibrational energy levels.

Using a value [44] of 25698.2 cm^{-1} for ν_{00} (CH), 25778.6 cm^{-1} for ν_{00} (ArCH), and a lower limit of 63.5 cm^{-1} for $D_o'(v = 0)$, a lower limit of 44 cm^{-1} is obtained for D_o''.

3.4 Rotational Term Values. Dubernet and coworkers [32, 34] have developed a general model describing the vibrational energy level structure of vdW complexes formed from the union of an RG atom and an open-shell diatom. For a complex in which the monomer can be described as a Hund's case (a) $^2\Pi$ state, both λ and σ, the projections of the diatom's electronic angular momentum (l) and spin angular momentum (s), respectively, remain coupled to the CH internuclear axis (r). Thus ω, the projection of the diatom's angular momentum (j) on r, is a well-defined quantum number of the complex ($\omega = \lambda + \sigma$). The basis set corresponding to this coupling scheme is given by the expression,

$$|\alpha,J,M_j,P,j,\omega,\pm\rangle = 2^{-1/2}\{|J,M_j,P\rangle\ |j,P,\omega,\rangle\ |\alpha,s,\sigma,\lambda\rangle \pm (-1)^{J-1/2}\ |J,M_j,-P\rangle \times |j,-P,-\omega\rangle|\alpha,s,-\sigma,-\lambda\rangle\}, \quad (4)$$

where α identifies the electronic state, J is the total angular momentum of the complex, M_j is the space fixed projection of J, P is the projection of J (and j) on r, and $\pm$ designates the parity of the levels. The projection quantum number P is analogous to K in a closed-shell system in the limit of a rigid T-shaped molecule.

The Hamiltonian is given by,

$$\mathbf{H} = \mathbf{H}^0_{mon} + \mathbf{H}'_{mon} + V_{inter} + B(J - j)^2 - D(J - j)^4 + ..., \quad (5)$$

where $(\mathbf{H}^0_{mon} + \mathbf{H}'_{mon})$ describes the rotation of the diatom at the free rotor limit, the term V_{inter} describes the intermolecular potential in which the diatom rotates, $B(J - j)^2$ is associated with the rotation of the whole complex, and the term $D(J - j)^4$ is associated with centrifugal distortion.

The matrix elements for an effective Hamiltonian, $\mathbf{H}^e$ derived by Chang and coworkers [21], are given by,

$$\mathbf{H}^e = \mathbf{H}_1 + \mathbf{H}_2 + \mathbf{H}_3 + \mathbf{H}_4, \quad (6)$$

where

$$\langle \mathbf{H}_1 \rangle = E_1 = B_\upsilon J(J+1) - D_\upsilon J^2(J+1)^2 + b_\upsilon[s(s+1) - \sigma^2 - P^2] + a\sigma\lambda \tag{7a}$$

$$\langle \mathbf{H}_2 \rangle = E_2 = (b_\upsilon + B_\upsilon)\, j\,(j+1) \tag{7b}$$

$$\langle \mathbf{H}_3 \rangle = \langle V_{inter} \rangle = \langle \Sigma_{l,m}\, V_{l,m}\,(R) C_m^{\,l}\,(\theta,0) \rangle \tag{7c}$$
$$= V_{1,0}\,\langle C_0^{\,1}(\theta,0) \rangle + V_{2,0}\,\langle C_0^{\,2}(\theta,0) \rangle + V_{2,2}\,\langle C_2^{\,2}(\theta,0) \rangle + \ldots$$

$$\langle \mathbf{H}_4 \rangle = -2\,\langle B\, J.j \rangle. \tag{7d}$$

In equations 7a–d, a and b_υ are the spin-orbit and rotational constant of CH, and $V_{l,m}$ (R) are coefficients of the renormalized spherical harmonics terms [$C_m^{\,l}$ (θ,0)] employed to approximate the average intermolecular potential.

Under our experimental conditions, the ArCH complex is generated in a free jet-cooled expansion with a temperature of approximately 10 K. Thus, it is presumed that only those states with $j = |\omega| = |P| = 1/2$ are populated. In the limit of free internal rotation, [$V_{1,0} = V_{2,m}$ (m = 0,2) = 0], diagonalization of the matrix yields rotational term values for these states that have the form $BN(N+1)$. Each end-over-end rotational state (N) correlates with a pair of degenerate (parity doublet) states:

$$2^{-1/2}\ \{\,|\alpha'',J,M_j,\pm 1/2,\ 1/2,\ \pm 1/2,\ \pm\rangle + |\alpha'',J,M_j,\pm 1/2,\ 1/2,\ \mp 1/2,\ \pm\rangle\}, \tag{8a}$$

where

$$J = N + 1/2,$$

and

$$2^{-1/2}\ \{\,|\alpha'',J,M_j,\pm 1/2,\ 1/2,\ \pm 1/2,\ \pm\rangle - |\alpha'',J,M_j,\pm 1/2,\ 1/2,\ \mp 1/2,\ \pm\rangle\}, \tag{8b}$$

where

$$J = N - 1/2.$$

The degeneracy of these two states is lifted for $V_{l,m}$ not equal to zero.

In the absence of Coriolis coupling, the rovibrational levels appear in degenerate pairs. Green and Lester [33] and Dubernet et al. [32] have shown that the splitting (ΔE) of the definite $P = 1/2$ levels of the same J but opposite parity should vary as $p(J+1/2)$. The magnitude of the splitting constant p is directly proportional to V_{dif} averaged over the vdW stretch vibrational wave function. Green and Lester [33] have derived an expression for p from third-order perturbation theory in the limit of small V_{dif}. In fact, this splitting is analogous to the Renner-Teller splitting in $K = 0$ vibronic levels of a linear triatomic $^2\Pi$ molecule, and is a direct measure of V_{dif}. Some years ago Hougen [45] showed how the splitting parameter p for these triatomic Renner-Teller systems can vary from $-2B$ to $+2B$. We follow Hougen's convention and define $\Delta E = E(J,F) - E(J,e)$. For p≈0, the case (a) limit, the rotational levels appear as closely spaced pairs of levels of the same J but opposite parity.

However, when $|p| \approx 2B$, the case (b) limit, the levels appear as closely spaced pairs of the same parity, with the same value of N, but with J differing by ±1. This is analogous to the level structure of a diatomic $^2\Sigma$ state. The lowest rotational level will have $J = 1/2$ and +(−) parity according to whether p is positive (negative). In the case (b) limit, the splitting between levels of the same N varies as γN. With some algebra, the case (b) spin splitting parameter γ can be expressed in terms of the case (a) parameter p as

$$\gamma = 2B+p \quad \text{for } p \approx -2B \ (^2\Sigma^- \text{ limit}), \tag{9a}$$

$$\gamma = 2B-p \quad \text{for } p \approx +2B \ (^2\Sigma^+ \text{ limit}). \tag{9b}$$

The empirically derived functional form of the splitting of the $J = \pm 1/2$ states, $\Delta(F_1,F_2) \propto \gamma(N+1/2)$, is particular to the case where the angular potential is dominated by the $V_{2,m}$ (m = 0,2) terms, and $V_{1,0}$ is approximately zero. In this case, the essential character of the eigenvectors (8a and 8b) is unchanged. Good agreement with the ground state structure was obtained using $V_{1,0} = 0$, $V_{2,2} = 0$, and $V_{2,0} = -22$ or $+29 \pm 1$ cm^{-1}. A comparison between the splittings determined from the experimental data and those calculated from this model is shown in Table 3. The value of $V_{2,0} = 29$ cm^{-1} is the same as that obtained by Heaven and coworkers [46] from calculations using the basis set and matrix elements given by Alexander [47]. They attribute the splitting of the levels to Coriolis coupling. This splitting is "Stark-like" and depends on the unassigned projection of j on the body-fixed axis. Both calculations were found to be sensitive to changes in $V_{2,0}$. Our calculations predict that on substitution of D for H for the ArCH

Table 3. Experimentally Determined and Calculated Ground State Rotational Energy Splittings of the ArCH Complex[a]

N	$\Delta\nu_{exp}$ [b]	$\Delta\nu_{cal}(CH)$ [c,d]
1	0.032	0.033
2	0.053	0.052
3	0.074	0.073
4	0.095	0.094
5	0.116	0.114
6	0.137	0.135
7	0.158	0.156

[a] In units of cm^{-1}.
[b] Experimental values determined from splitting constant.
[c] Calculated based on model described in text.
[d] Calculated based on model calculations performed by Heaven and coworkers [46] using the Hamiltonian given by the equation,

$$H_{ang} = H_{CH} + L^2/(2m\mu\langle R^2\rangle) + V(\theta) \text{ where } V(\theta) = V_1\cos(\theta) + V_2/2(3\cos^2(\theta)-1),$$

and basis set and matrix elements given by Alexander [47].

complex, the splitting will not be the same if $V_{2,m}$ (m = 0,2) are the same for the ArCD. Measurement of this splitting in the ArCD complex is reported elsewhere [48].

3.5 Excited and Ground State Geometries. The correlation diagrams demonstrating how the free-rotor energy levels of the diatom in either a Π or Σ electronic configuration transform with respect to an increase in the strength of RG-monomer interaction are an important result of the free-rotor model described by Dubernet and coworkers. The model also provides an estimate for the barrier to internal rotation for ArCH if bend/stretching coupling is neglected. In this limit, the angular dependence of the potential energy is periodic and may be expressed in terms of $V_{l,m}$. For $V_{10} = V_{22} = 0$, a positive K value corresponds to a T-shaped geometry while a negative value corresponds to a linear geometry. For the excited state of ArCH, the anisotropy of the intermolecular potential is reflected in the difference between the (0,0°,0) and (0,1°,0) energy levels. Using this model, the rotational constant for CH (b = 12.645 cm^{-1}), and reasonable values for V_{10} and V_{20} (i.e., less than the dissociation energy, implying ($-10b' \leq V_{i0} \leq 10b$)), a separation between (0,0°,0) and (0,1°,0) of less than 2b is indicative of a linear geometry for the excited state of the ArCH complex. The (0,0°,0) and (0,1°,0) bands of the ArCH

complex are located at 25,778.6 cm^{-1} and 25,794.3 cm^{-1}, respectively. If the proposed vibrational assignments are correct, then the upper state is linear, since the difference in energy between these bands (16.0 cm^{-1}) is considerably less than 2b (25.3 cm^{-1}). The nature of the ArCH ground state intermolecular potential is reflected in the observed splitting of the ground state rotational energy levels. Unfortunately, the equilibrium geometry of the ground state cannot be determined from the rotational energy level splittings alone, because $V_{2,m}$ is not uniquely characterized by a fit to the splitting.

The geometry of the ground state can, however, be inferred from an examination of its rovibronic transitions and the correlation diagrams of Dubernet and coworkers. In the case of ArOH, the transitions from the vibrationless ground state $(0,0^0,0)$ to the electronically excited state associated with the OH($A^2\Sigma^+$) state yield P, Q, and R branches analogous to an OH $A^2\Sigma$-$X^2\Pi$ band. Thus, the geometry of the ground state is consistent with the model described by Dubernet and coworkers in the linear case limit. That is, the principal axes of symmetry ($C_{\infty,v}$) of the complex and diatom are coincident, indicating that the projection of the total orbital angular momentum and the total spin angular momentum of OH coincide with the principal axis of the complex. Therefore, the vibrationless ground state of the complex is analogous to Hund's case (a) $^2\Pi$ diatom. In contrast, all of the ArCH system's rovibronic bands observed reveal the presence of only the P and R branches; the Q branch being missing or very weak. The observed Σ-Σ like structure is thus indicative of a *parallel* transition of a near-symmetric top molecule with $\Delta K = 0$ and $\Delta N = \pm 1$. Using the correlation diagrams obtained from the model of Dubernet and coworkers, transitions for a state of Σ symmetry is indicative of the vdW complex having a T-shape structure. In the limiting case of this configuration, there is no longer a true $C_{\infty,v}$ axis of symmetry through the molecule and, as a result, the parity in the electronic structure is lost. Thus, the parity of the total wavefunction is determined solely by the rotational wavefunction. The correlation diagrams of Dubernet and coworkers always show that the lowest energy levels on the T-shaped side correspond to the lowest projection on the principal axis from the diatom.

3.6 Metastable Levels and Dissociative Continuum. An interesting feature of the ArCH spectra is the dissociative continua. As in ArNO, the inner repulsive wall of the upper state is sampled from the minimum of the ground state potential well. Thus, the Franck-Condon factors for the bound-bound transitions from the vibrationless ground state increase in the direction of the continuum, towards higher energy, and the best overlap is in the bound-unbound region of the spectra. If, in fact, the observed ArCH transitions do involve a change in geometry, then the best estimate of the Franck-Condon factors would

require a three-dimensional representation of the potentials including the angular dependence as well as Ar-CH bond length.

3.7 Predissociation. The LIF spectra of ArCH in the vicinity of the CH (1,0) band were recorded by monitoring the fluorescence near either the CH (1,0) or (1,1) band. When attempts were made to monitor the LIF signal near the (0,0) CH band, as was done in previous ArOH and KrOH experiments [26], a continuous fluorescence signal, which we presume is associated with fluorescence from the CH B(v′=0) level, is observed. The signal had a slight wavelength dependence, which appeared to follow the dye curve. For the ArOH complex, excitation near the OH (1,0) band results in OH emission near its (0,0) band. The emission from OH (v′ = 0) occurs because the vibrational predissociation rate, τ_{vp}, for

$$\text{Ar-OH}(1, r^{\rho}, v_s) \rightarrow \text{OH}(A,\upsilon = 0) + \text{Ar}, \tag{10}$$

is considerably faster than the radiative decay rates, τ_{Rad},

$$\text{Ar-OH}(1, r^{\rho}, v_s) \rightarrow \text{Ar-OH}(X) + h\nu, \tag{11}$$

for $\upsilon_1 = 1$. Berry and coworkers [16] reported vibrational predissociation rates for ArOH $(1,0^0,v_s)$ ranging from $\tau_{vp} \geq 17$ to 156 ps. These are considerably faster than the radiative decay rates of ArOH $(1,0^0,v_s)$, which are expected to be close to that of the uncomplexed OH fragment (τ_{Rad} = 715 to 740 ns). If the vibrational predissociation rates of ArCH are closer to that of NeOH, which range in value [24] from τ_{Rad} = 1.7 to 2.5 μs for $\upsilon_1 = 1$, then it would not be surprising that the best fluorescence signals from the ArCH $(1, r^{\rho}, v_s)$ vibrational levels are collected near the CH $B^2\Sigma^- - X^2\Pi_r$ (1,0) and (1,1) electronic bands. It may be that the fluorescence was a result of the probe laser photolyzing the precursor.

4. SUMMARY/CONCLUSION

Gas-phase ArCH complexes have been detected by LIF in the region of CH $B^2\Sigma^- - X^2\Pi_r$ (0,0) and (1,0) transitions. The excitation spectra reveal a number of features that were assigned to stretching or bending motions of the ArCH complex. Rotational analysis of eight of the rovibronic bands reveals that the vdW bond length in the complex is increased by approximately 23% upon electronic excitation. A nonnegligible splitting of the ground state rotational levels is also observed. In addition to the rotational constants, lower limits of the ground and excited state binding energies were estimated. A linear

equilibrium geometry for the excited state and a T-shaped geometry for the ground state is inferred from an analysis of the rotational spectra in terms of the free rotor model developed by Dubernet and coworkers.

INTENTIONALLY LEFT BLANK.

5. REFERENCES

1. Bernath, P., C. Brazier, T. Olsen, R. Hailey, W. Fernando, C. Woods, and J. Hardwick. Journal of Molecular Spectroscopy, vol. 147, pp. 16–26, 1991.

2. Bernath, P. Journal of Chemical Physics, vol. 86, p. 4838, 1987.

3. Stanton, C., N. Garland, and H. Nelson. Journal of Physical Chemistry, vol. 95, p. 1277, 1991.

4. Gaydon, A., and H. Wolfhard. Flames, New York: Wiley, 1979.

5. Berman, M., J. Fleming, and M. Lin. Proc. Int. Symp. Combust., vol. 19, p. 73, 1982.

6. Finlayson-Pitts, B., and J. Pitts, Jr. Atmospheric Chemistry, Wiley: New York, 1986.

7. Rydbeck, O., J. Ellder, and W. Irvine. Nature, vol. 246, p. 4666, 1973.

8. Brooks, B., and H. Schaeffer. Journal of Chemical Physics, vol. 67, p. 5146, 1977.

9. Dunning, T., L. Harding, R. Bair, R. Eades, and R. Shepard. Journal of Physical Chemistry, vol. 90, p. 344, 1986.

10. Hutson, J. Annual Review of Physical Chemistry, vol. 41, p. 123, 1990.

11. Berry, M., R. Loomis, L. Giancarlo, and M. Lester. Journal of Chemical Physics, vol. 96, p. 7890, 1992.

12. Goodman, J., and L. Brus. Journal of Chemical Physics, vol. 67, p. 4858, 1977.

13. Fawzy, W., and M. Heaven. Journal of Chemical Physics, vol. 89, p. 7030, 1988.

14. Berry, M., M. Brustein, J. Adamo, and M. Lester. Journal of Physical Chemistry, vol. 92, p. 5551, 1988.

15. Berry, M., M. Brustein, and M. Lester. Chemical Physics Letters, vol. 153, p. 17, 1988.

16. Berry, M., M. Brustein, and M. Lester. Journal of Chemical Physics, vol. 92, p. 6469, 1990.

17. Schleipen, J., L. Nemes, J. Heinze, and J. ter Meulen. Chemical Physics Letters, vol. 175, p. 561, 1990.

18. Fawzy, W., and M. Heaven. Journal of Chemical Physics, vol. 92, p. 909, 1990.

19. Bramble, S., and P. Hamilton. Chemical Physics Letters, vol. 170, p. 107, 1990.

20. Ohshima, Y., M. Lida, and Y. Endo. Journal of Chemical Physics, vol. 95, p. 7001, 1991.

21. Chang, B., L. Lu, D. Cullin, B. Rehfuss, J. Williamson, T. Miller, W. Fawzy, X. Zheng, S. Fei, and M. Heaven. Journal of Chemical Physics, vol. 95, p. 7086, 1991.

22. Schnupf, U., J. Bowman, and M. Heaven. Chemical Physics Letters, vol. 189, p. 487, 1992.

23. Lin, Y., S. Kulkarni, and M. Heaven. Journal of Physical Chemistry, vol. 94, p. 1720, 1990.

24. Lin, Y., S. Fei, X. Zheng, and M. Heaven. Journal of Chemical Physics, vol. 96, p. 5020, 1992.

25. Chang, B., J. Cullin, J. Williamson, J. Dunlop, B. Rehfuss, and T. Miller. Journal of Chemical Physics, vol. 96, p. 3476, 1992.

26. Lemire, G., and R. Sausa. Journal of Physical Chemistry, vol. 96, p. 4821, 1992.

27. Fei, S., X. Zheng and M. Heaven. Journal of Chemical Physics, vol. 97, p. 1655, 1992.

28. Fawzy, W., and J. Hougen. Journal of Molecular Spectroscopy, vol. 137, p. 154, 1989.

29. Degli-Esposti, A., and H. Werner. Journal of Chemical Physics, vol. 93, p. 3351, 1990.

30. Chakravarty, C., D. Clary, A. Degli Esposti, and H. Werner. Journal of Chemical Physics, vol. 93, p. 3367, 1990.

31. Chakravarty, C., D. Clary, A. Degli Esposti, and H. Werner. Journal of Chemical Physics, vol. 95, p. 8149, 1991.

32. Dubernet, M., D. Flower, and J. Hutson. Journal of Chemical Physics, vol. 94, p. 7602, 1991.

33. Green, W., Jr., and M. Lester. Journal of Chemical Physics, vol. 96, p. 2573, 1992.

34. Dubernet, M., P. Tuckey, and J. Hutson. Chemical Physics Letters, vol. 193, p. 355, 1992.

35. Langridge-Smith, P., E. Carrasquillo, and D. Levy. Journal of Chemical Physics, vol. 74, p. 6513, 1981.

36. Sato, K., Y. Achiba, and K. Kimura. Journal of Chemical Physics, vol. 81, p. 57, 1984.

37. Mills, P., C. Western, and B. Howard. Journal of Physical Chemistry, vol. 90, p. 4961, 1986.

38. Miller, J. Journal of Chemical Physics, vol. 86, p. 3166, 1987.

39. Miller, J. Journal of Chemical Physics, vol. 90, p. 4031, 1989.

40. Smith, D., and J. Miller. Journal of Chemical Society: Faraday Trans., vol. 86, p. 2441, 1990.

41. Lin, Y., and M. Heaven. Journal of Chemical Physics, vol. 94, p. 5765, 1991.

42. Randall, R., C. Chuang, and M. Lester. Chemical Physics Letters, vol. 200, p. 113, 1992.

43. Gerö, L. Z. Phys., vol. 118, p. 27, 1921.

44. Huber, K., and G. Herzberg. Molecular Spectra and Molecular Structure IV. New York: Van Nostrand Reinhold Company. Constants of Diatomic Molecules, 1979.

45. Hougen, J. T. Journal of Chemical Physics, vol. 36, p. 519, 1962.

46. Heaven, M. Private communication.

47. Alexander, M. Journal of Chemical Physics, vol. 76, p. 5974, 1982.

48. McQuaid, M. J., G. W. Lemire, and R. C. Sausa. Chemical Physics Letters, vol. 210, p. 350, 1993.

INTENTIONALLY LEFT BLANK.

NO. OF COPIES	ORGANIZATION
2	DEFENSE TECHNICAL INFO CTR ATTN DTIC DDA 8725 JOHN J KINGMAN RD STE 0944 FT BELVOIR VA 22060-6218
1	DIRECTOR US ARMY RESEARCH LAB ATTN AMSRL CS AL TP 2800 POWDER MILL RD ADELPHI MD 20783-1145
1	DIRECTOR US ARMY RESEARCH LAB ATTN AMSRL CS AL TA 2800 POWDER MILL RD ADELPHI MD 20783-1145
3	DIRECTOR US ARMY RESEARCH LAB ATTN AMSRL CI LL 2800 POWDER MILL RD ADELPHI MD 20783-1145
	ABERDEEN PROVING GROUND
2	DIR USARL ATTN AMSRL CI LP (305)

NO. OF COPIES	ORGANIZATION
1	HQDA ATTN SARD TT DR F MILTON PENTAGON WASHINGTON DC 20310-0103
1	HQDA ATTN SARD TT MR J APPEL PENTAGON WASHINGTON DC 20310-0103
1	HQDA OASA RDA ATTN DR C H CHURCH PENTAGON ROOM 3E486 WASHINGTON DC 20310-0103
4	COMMANDER US ARMY RESEARCH OFFICE ATTN R GHIRARDELLI D MANN R SINGLETON R SHAW P O BOX 12211 RESEARCH TRIANGLE PARK NC 27709-2211
1	DIRECTOR ARMY RESEARCH OFFICE ATTN AMXRO RT IP LIB SERVICES P O BOX 12211 RESEARCH TRIANGLE PARK NC 27709-2211
2	COMMANDER US ARMY ARDEC ATTN SMCAR AEE B D S DOWNS PICATINNY ARSENAL NJ 07806-5000
2	COMMANDER US ARMY ARDEC ATTN SMCAR AEE J A LANNON PICATINNY ARSENAL NJ 07806-5000
1	COMMANDER US ARMY ARDEC ATTN SMCAR AEE BR L HARRIS PICATINNY ARSENAL NJ 07806-5000

NO. OF COPIES	ORGANIZATION
2	COMMANDER US ARMY MISSILE COMMAND ATTN AMSMI RD PR E A R MAYKUT AMSMI RD PR P R BETTS REDSTONE ARSENAL AL 35809
1	OFFICE OF NAVAL RESEARCH DEPARTMENT OF THE NAVY ATTN R S MILLER CODE 432 800 N QUINCY STREET ARLINGTON VA 22217
1	COMMANDER NAVAL AIR SYSTEMS COMMAND ATTN J RAMNARACE AIR 54111C WASHINGTON DC 20360
2	COMMANDER NAVAL SURFACE WARFARE CENTER ATTN R BERNECKER R 13 G B WILMOT R 16 SILVER SPRING MD 20903-5000
4	COMMANDER NAVAL RESEARCH LABORATORY ATTN J MCDONALD E ORAN J SHNUR R J DOYLE CODE 6110 WASHINGTON DC 20375
2	COMMANDER NAVAL WEAPONS CENTER ATTN T BOGGS CODE 388 T PARR CODE 3895 CHINA LAKE CA 93555-6001
1	SUPERINTENDENT NAVAL POSTGRADUATE SCHOOL DEPT OF AERONAUTICS ATTN D W NETZER MONTEREY CA 93940
3	AL LSCF ATTN R CORLEY R GEISLER J LEVINE EDWARDS AFB CA 93523-5000

NO. OF COPIES	ORGANIZATION
1	AFOSR ATTN J M TISHKOFF BOLLING AIR FORCE BASE WASHINGTON DC 20332
1	OSD SDIO IST ATTN L CAVENY PENTAGON WASHINGTON DC 20301-7100
1	COMMANDANT USAFAS ATTN ATSF TSM CN FORT SILL OK 73503-5600
2	UNIV OF DAYTON RSCH INST ATTN D CAMPBELL AL PAP EDWARDS AFB CA 93523
1	NASA LANGLEY RESEARCH CENTER ATTN G B NORTHAM MS 168 LANGLEY STATION HAMPTON VA 23365
4	NATL BUREAU OF STANDARDS US DEPT OF COMMERCE ATTN J HASTIE M JACOX T KASHIWAGI H SEMERJIAN WASHINGTON DC 20234
2	DIRECTOR LLNL ATTN C WESTBROOK W TAO MS L 282 P O BOX 808 LIVERMORE CA 94550
1	DIRECTOR LOS ALAMOS NATL LAB ATTN B NICHOLS T7 MS B284 P O BOX 1663 LOS ALAMOS NM 87545

NO. OF COPIES	ORGANIZATION
3	DIRECTOR SANDIA NATL LABS DIVISION 8354 ATTN S JOHNSTON P MATTERN D STEPHENSON LIVERMORE CA 94550
1	BRIGHAM YOUNG UNIV DEPT OF CHEMICAL ENGNRG ATTN M W BECKSTEAD PROVO UT 84058
1	CALIF INSTITUTE OF TECH JET PROPULSION LAB ATTN L STRAND MS 125 224 4800 OAK GROVE DRIVE PASADENA CA 91109
1	CALIF INST OF TECHNLGY ATTN F E C CULICK MC 301 46 204 KARMAN LAB PASADENA CA 91125
1	UNIV OF CALIF LOS ALAMOS SCIENTIFIC LAB P O BOX 1663 MAIL STOP B216 LOS ALAMOS NM 87545
1	UNIV OF CALIF BERKELEY CHEMISTRY DEPT ATTN C BRADLEY MOORE 211 LEWIS HALL BERKELEY CA 94720
1	UNIV OF CALIF SAN DIEGO ATTN F A WILLIAMS AMES B010 LA JOLLA CA 92093
2	UNIV OF CALIF SANTA BARBARA QUANTUM INSTITUTE ATTN K SCHOFIELD M STEINBERG SANTA BARBARA CA 93106
3	UNIV OF SOUTHERN CALIF DEPT OF CHEMISTRY ATTN R BEAUDET S BENSON C WITTIG LOS ANGELES CA 90007

NO. OF COPIES	ORGANIZATION
1	CORNELL UNIVERSITY DEPT OF CHEMISTRY ATTN T A COOL BAKER LABORATORY ITHACA NY 14853
1	UNIV OF DELAWARE CHEMISTRY DEPT ATTN T BRILL NEWARK DE 19711
1	UNIV OF FLORIDA DEPT OF CHEMISTRY ATTN J WINEFORDNER GAINESVILLE FL 32611
1	THE JOHNS HOPKINS UNIV CPIA ATTN T W CHRISTIAN 10630 LITTLE PATUXENT PKWY SUITE 202 COLUMBIA MD 21044-3200
1	UNIV OF MINNESOTA DEPT OF MECHANICAL ENGNRNG ATTN E FLETCHER MINNEAPOLIS MN 55455
1	PURDUE UNIV SCHL OF AERONAUTICS AND ASTRONAUTICS ATTN J R OSBORN GRISSOM HALL WEST LAFAYETTE IN 47906
1	PURDUE UNIV DEPT OF CHEMISTRY ATTN E GRANT WEST LAFAYETTE IN 47906
2	PURDUE UNIV SCHL OF MECHANICAL ENGNRNG ATTN N M LAURENDEAU S N B MURTHY TSPC CHAFFEE HALL WEST LAFAYETTE IN 47906
1	RENSSELAER POLYTECHNIC INST DEPT OF CHEMICAL ENGNRNG ATTN A FONTIJN TROY NY 12181

NO. OF COPIES	ORGANIZATION
1	STANFORD UNIVERSITY DEPT OF MECHANICAL ENGNRNG ATTN R HANSON STANFORD CA 94305
1	UNIV OF TEXAS DEPT OF CHEMISTRY ATTN W GARDINER AUSTIN TX 78712
1	VA POLYTECH INST AND STATE UNIV ATTN J A SCHETZ BLACKSBURG VA 24061
1	APPLIED COMBUSTION TECHNLGY INC ATTN A M VARNEY P O BOX 607885 ORLANDO FL 32860
2	APPLIED MECHANICS REVIEWS ASME ATTN R E WHITE A B WENZEL 345 E 47TH STREET NEW YORK NY 10017
1	BATTELLE TWSTIAC 505 KING AVENUE COLUMBUS OH 43201-2693
1	COHEN PROFESSIONAL SERVICES ATTN N S COHEN 141 CHANNING STREET REDLANDS CA 92373
1	EXXON RESEARCH & ENG CO ATTN A DEAN ROUTE 22E ANNANDALE NJ 08801
1	GEN APPLD SCIENCE LABS INC 77 RAYNOR AVENUE RONKONKAMA NY 11779-6649
1	GEN MOTORS RSCH LABS PHYSICAL CHEMISTRY DEPARTMENT ATTN T SLOANE WARREN MI 48090-9055

NO. OF COPIES	ORGANIZATION
2	HERCULES INC ATTN W B WALKUP E A YOUNT P O BOX 210 ROCKET CENTER WV 26726
1	HERCULES INC ATTN R V CARTWRIGHT 100 HOWARD BLVD KENVIL NJ 07847
1	ALLIANT TECHSYSTEMS INC MARINE SYSTEMS GROUP ATTN D E BRODEN MS MN50 2000 600 2ND STREET NE HOPKINS MN 55343
1	ALLIANT TECHSYSTEMS INC ATTN R E TOMPKINS MN 11 2720 600 SECOND ST NORTH HOPKINS MN 55343
1	IBM CORPORATION RESEARCH DIVISION ATTN A C TAM 5600 COTTLE ROAD SAN JOSE CA 95193
1	IIT RESEARCH INSTITUTE ATTN R F REMALY 10 WEST 35TH STREET CHICAGO IL 60616
1	LOCKHEED MISSILES AND SPACE CO ATTN GEORGE LO 3251 HANOVER STREET DEPT 52 35 B204 2 PALO ALTO CA 94304
1	OLIN ORDNANCE ATTN V MCDONALD LIBRARY P O BOX 222 ST MARKS FL 32355-0222
1	SCIENCE APPLICATIONS INC ATTN R B EDELMAN 23146 CUMORAH CREST WOODLAND HILLS CA 91364

NO. OF COPIES	ORGANIZATION
3	SRI INTERNATIONAL ATTN G SMITH D CROSLEY D GOLDEN 333 RAVENSWOOD AVENUE MENLO PARK CA 94025
1	STEVENS INSTITUTE OF TECH DAVIDSON LABORATORY ATTN R MCALEVY III HOBOKEN NJ 07030
1	SVERDRUP TECHNLGY INC LERC GROUP ATTN R J LOCKE MS SVR 2 2001 AEROSPACE PARKWAY BROOK PARK OH 44142
3	THIOKOL CORPORATION ELKTON DIVISION ATTN R BIDDLE R WILLER TECH LIB P O BOX 241 ELKTON MD 21921
3	THIOKOL CORPORATION WASATCH DIVISION ATTN S J BENNETT P O BOX 524 BRIGHAM CITY UT 84302
1	UNITED TECH RSCH CTR ATTN A C ECKBRETH EAST HARTFORD CT 06108
1	UNITED TECH CORP CHEMICAL SYS DIV ATTN R R MILLER P O BOX 49028 SAN JOSE CA 95161-9028
1	UNIVERSAL PROPULSION CO ATTN H J MCSPADDEN 25401 NORTH CENTRAL AVENUE PHOENIX AZ 85027-7837

NO. OF COPIES	ORGANIZATION
3	ALLIANT TECHSYSTEMS ATTN C CANDLAND L OSGOOD R BECKER 600 SECOND ST NE HOPKINS MN 55343

NO. OF COPIES	ORGANIZATION
	ABERDEEN PROVING GROUND
37	DIR USARL ATTN: AMSRL-WT-P, A HORST AMSRL-WT-PA, T MINOR M MCQUAID (10 CPS) AMSRL-WT-PC, R A FIFER G F ADAMS W R ANDERSON R A BEYER S W BUNTE C F CHABALOWSKI R DANIEL B E FORCH A J KOTLAR K L MCNESBY A W MIZIOLEK J B MORRIS R A PESCE-RODRIGUEZ B M RICE R C SAUSA (10 CPS) J A VANDERHOFF

USER EVALUATION SHEET/CHANGE OF ADDRESS

This Laboratory undertakes a continuing effort to improve the quality of the reports it publishes. Your comments/answers to the items/questions below will aid us in our efforts.

1. ARL Report Number/Author ARL-TR-1220 (McQuaid) Date of Report October 1996

2. Date Report Received _____

3. Does this report satisfy a need? (Comment on purpose, related project, or other area of interest for which the report will be used.) _____

4. Specifically, how is the report being used? (Information source, design data, procedure, source of ideas, etc.) _____

5. Has the information in this report led to any quantitative savings as far as man-hours or dollars saved, operating costs avoided, or efficiencies achieved, etc? If so, please elaborate. _____

6. General Comments. What do you think should be changed to improve future reports? (Indicate changes to organization, technical content, format, etc.) _____

CURRENT ADDRESS

_____
Organization

_____
Name

_____
Street or P.O. Box No.

_____
City, State, Zip Code

7. If indicating a Change of Address or Address Correction, please provide the Current or Correct address above and the Old or Incorrect address below.

OLD ADDRESS

_____
Organization

_____
Name

_____
Street or P.O. Box No.

_____
City, State, Zip Code

(Remove this sheet, fold as indicated, tape closed, and mail.)
(DO NOT STAPLE)

DEPARTMENT OF THE ARMY

OFFICIAL BUSINESS

NO POSTAGE
NECESSARY
IF MAILED
IN THE
UNITED STATES

BUSINESS REPLY MAIL
FIRST CLASS PERMIT NO 0001,APG,MD

POSTAGE WILL BE PAID BY ADDRESSEE

DIRECTOR
U S ARMY RESEARCH LABORATORY
ATTN AMSRL WT PA
ABERDEEN PROVING GROUND MD 21005-5066